

## Nuclear shapes of $^{24}\text{Mg}$ and $^{28}\text{Si}$ by inelastic scattering of $^{12}\text{C}$ and $^{16,18}\text{O}^\dagger$

John S. Eck, D. O. Elliott,\* and W. J. Thompson†

*Department of Physics, Kansas State University, Manhattan, Kansas 66506*

F. Todd Baker

*Department of Physics and Astronomy, The University of Georgia, Athens, Georgia 30602*

(Received 23 May 1977)

The measurement and analysis of the differential cross sections for the elastic and inelastic scattering to the lowest  $2^+$  states of  $^{24}\text{Mg}$  and  $^{28}\text{Si}$  in the scattering of  $^{12}\text{C}$  at bombarding energies of 25 and 30 MeV are reported. In addition, elastic and inelastic scattering for  $^{16}\text{O} + ^{24}\text{Mg}$ ,  $^{16}\text{O} + ^{28}\text{Si}$ , and  $^{18}\text{O} + ^{28}\text{Si}$ , which had been measured previously, are reanalyzed. The analyses are carried out utilizing a coupled-channels code, and deformation lengths for  $^{24}\text{Mg}$  and  $^{28}\text{Si}$  are determined from the scattering of the different projectiles. The deformation lengths extracted from these analyses are compared with each other and with the results of a recently reported systematic investigation of deformation lengths in light nuclei.

NUCLEAR REACTIONS  $^{24}\text{Mg}(^{12}\text{C}, ^{12}\text{C})$ ,  $^{24}\text{Mg}(^{12}\text{C}, ^{12}\text{C})$   $^{24}\text{Mg}^* Q = -1.37$  MeV,  $E = 25$  and  $30$  MeV;  $^{24}\text{Mg}(^{16}\text{O}, ^{16}\text{O})$ ,  $^{24}\text{Mg}(^{16}\text{O}, ^{16}\text{O})$   $^{24}\text{Mg}^* Q = -1.37$  MeV,  $E = 36$  MeV;  $^{28}\text{Si}(^{12}\text{C}, ^{12}\text{C})$ ,  $^{28}\text{Si}(^{12}\text{C}, ^{12}\text{C})$   $^{28}\text{Si}^* Q = -1.78$  MeV,  $E = 25$  and  $30$  MeV;  $^{28}\text{Si}(^{16}\text{O}, ^{16}\text{O})$ ,  $^{28}\text{Si}(^{16}\text{O}, ^{16}\text{O})$   $^{28}\text{Si}^* Q = -1.78$  MeV,  $E = 33, 36,$  and  $38$  MeV;  $^{28}\text{Si}(^{18}\text{O}, ^{18}\text{O})$   $^{28}\text{Si}(^{18}\text{O}, ^{18}\text{O})$   $^{28}\text{Si}^* Q = -1.78$  MeV,  $E = 36$  MeV, measured  $\sigma(\theta)$ ,  $\theta_{\text{lab}} = 10-70$ ; deduced optical model parameters and nuclear deformation lengths, compared deformation lengths with systematics.

### I. INTRODUCTION

The inelastic scattering of heavy ions at energies near the Coulomb barrier can yield information on interference between nuclear and Coulomb scattering,<sup>1-7</sup> and can therefore be used to investigate differences between the nuclear potential and charge distributions.<sup>8</sup> This technique has been extensively used for rare-earth nuclei to compare  $\alpha$  inelastic scattering<sup>1</sup> with  $\alpha$ -induced Coulomb excitation<sup>9</sup> and electron inelastic scattering.<sup>10</sup> However, it has seldom been applied to light nuclei.<sup>4,11,12</sup> The available analyses suggest that nuclear potential and charge distributions in nuclei with  $A \leq 28$  are essentially equal.<sup>13</sup>

Although the elastic scattering of heavy ions has been studied in some detail and much systematic information has been accumulated,<sup>14</sup> the inelastic scattering of heavy ions has received little attention and, except for Coulomb excitation, no detailed systematic studies have been carried out. Experimentally, it is difficult to extract the inelastic-scattering peaks in the presence of the dominant elastic scattering. Theoretical difficulties arise in calculations involving the long-range inelastic Coulomb interaction, with the consequent necessity of including many partial waves. Often, as here, there is such strong coupling between the elastic and inelastic channels that the distorted-waves Born approximation (DWBA) is inappropriate,

and a coupled-channels (CC) analysis must be performed, which requires long computing times.

Here we report the measurement and analysis of differential cross sections for elastic and inelastic scattering to the lowest  $2^+$  states of  $^{24}\text{Mg}$  and  $^{28}\text{Si}$  in the scattering of  $^{12}\text{C}$  at bombarding energies of 25 and 30 MeV. The experimental details are discussed in Sec. II. In addition, elastic and inelastic scattering for  $^{16}\text{O} + ^{24}\text{Mg}$ ,  $^{16}\text{O} + ^{28}\text{Si}$ , and  $^{18}\text{O} + ^{28}\text{Si}$ , the measurement of which has been previously reported,<sup>15,16</sup> are reanalyzed. As pointed out by the original authors, the CC analysis did not properly include Coulomb excitation, so that the analyses of the forward-angle inelastic cross sections were inappropriate in some cases. The CC analysis of the present and previous data, including Coulomb excitation correctly, is presented in Sec. III. In Sec. IV, potential deformation parameters for  $^{24}\text{Mg}$  and  $^{28}\text{Si}$  are extracted and their dependence on bombarding energy and projectile size is treated. The results of this study are discussed and summarized in Sec. V.

### II. EXPERIMENT

The 25-MeV  $^{12}\text{C}$  beam was obtained as  $\text{CN}^+$  from a diode ion source using a mixture of  $\text{CH}_4$  and  $\text{N}_2$  as the source gas.<sup>17</sup> It was accelerated using the Kansas State University Model EN tandem accelerator, and the  $^{12}\text{C}(4+)$  charge-state component of

the beam was utilized. The 30-MeV  $^{12}\text{C}$  beam was obtained by direct extraction of a  $\text{C}^-$  beam from the diode source using CO as a source gas,<sup>18</sup> and selection of the  $^{12}\text{C}(5+)$  beam component. Typical beam currents incident on target were 50–150 mA.

The  $^{24}\text{Mg}$  targets were made by reducing MgO (enriched to 99.6% in  $^{24}\text{Mg}$ ) with Zr metal and evaporating the resulting Mg metal onto 10- $\mu\text{g}/\text{cm}^2$  carbon foils.<sup>19</sup> The target thicknesses ranged from 50–120  $\mu\text{g}/\text{cm}^2$  of  $^{24}\text{Mg}$ . These targets also contained a trace amount of Zr which was used for relative normalization. The  $^{28}\text{Si}$  targets consisted of self-supporting foils of  $\text{SiO}_2$  (enriched to >99.4%  $^{28}\text{Si}$ ) and ranged from 100 to 150  $\mu\text{g}/\text{cm}^2$  in thickness. The  $\text{SiO}_2$  targets were fabricated by evaporation of  $\text{SiO}_2$  from a tungsten (W) boat and thereby contained a trace amount of W which was useful for normalization purposes.

The scattered particles were detected using an array of four 100- $\mu\text{m}$  Si surface-barrier detectors. The angular distributions were measured in the laboratory angular range from 12.5° to 65°. The data were accumulated in singles mode using standard electronics. A typical channel spectrum for  $^{12}\text{C} + ^{24}\text{Mg}$  scattering shown in Fig. 1 indicates

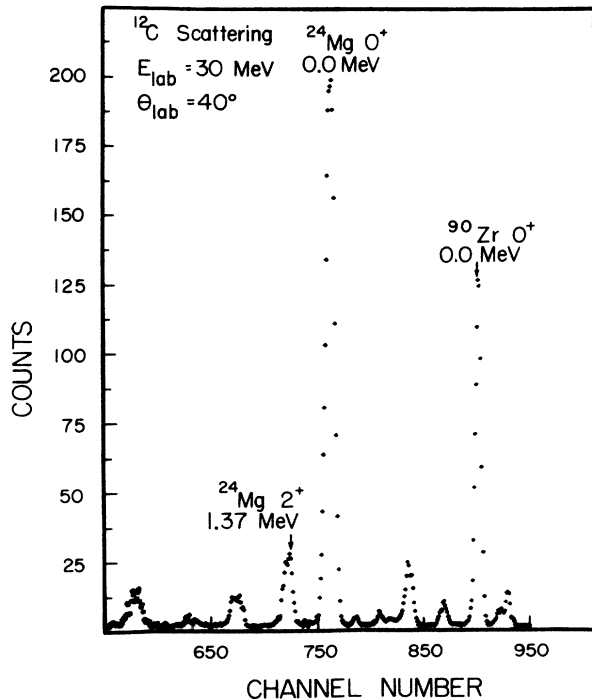


FIG. 1. Typical pulse-height spectrum;  $^{12}\text{C} + ^{24}\text{Mg}$  scattering at a  $^{12}\text{C}$  lab bombarding energy  $E_{\text{lab}} = 30$  MeV and a scattering angle  $\theta_{\text{lab}} = 40^\circ$ . The elastic and inelastic ( $Q = -1.37$  MeV) scattering peaks are well resolved, so that the yields are easily extracted. The  $^{90}\text{Zr}$  scattering was used to obtain relative normalizations, as discussed in Sec. II.

good separation of elastic and inelastic peaks, unlike the channel spectra obtained in the Coulomb-nuclear interference energy region of  $\alpha$  scattering from rare-earth nuclei,<sup>1</sup> in which elastic and inelastic scattering are unresolved, and therefore require special spectrum-shape analyses to separate inelastic from elastic yields.

By determining the relative yields of the  $^{12}\text{C} + ^{24}\text{Mg}$  elastic and inelastic ( $Q = -1.37$  MeV) scattering to the  $^{12}\text{C} + ^{90}\text{Zr}$  elastic scattering, and by assuming that the  $^{12}\text{C} + ^{90}\text{Zr}$  scattering is pure Rutherford, the relative  $^{12}\text{C} + ^{24}\text{Mg}$  elastic and inelastic cross sections were obtained. The relative normalization is accurate to <2% for the elastic scattering and to <5% for the inelastic scattering. The absolute normalization was obtained by assuming that the  $^{12}\text{C} + ^{24}\text{Mg}$  elastic scattering at the most forward angles is pure Rutherford scattering, as is justified by optical-model calculations. The absolute cross sections are estimated to have an accuracy  $\sim 10\%$ . The relative and absolute cross sections for  $^{12}\text{C} + ^{28}\text{Si}$  were obtained similarly, using the scattering of the projectile from the W impurity present in the  $\text{SiO}_2$  targets to obtain the relative normalization of the cross section at the various angles. The cross section measurements for  $^{18}\text{O} + ^{24}\text{Mg}$  are described in Ref. 15, and those for  $^{16}\text{O} + ^{28}\text{Si}$  and  $^{18}\text{O} + ^{28}\text{Si}$  are in Ref. 16. The experimental cross sections are shown in Figs. 2–6. Tabulations of the cross sections are obtainable from Eck.

### III. ANALYSIS

The elastic- and inelastic differential cross sections were fitted using a deformed optical-model (OM) potential of a form appropriate to a model of the target nuclei as axially symmetric rotors<sup>20,21</sup>

$$V = - \frac{V_0}{1 + \exp[(r - R')/a_0]} - i \frac{W_0}{[1 + \exp[(r - R')/a_w]]} + V_c(r), \quad (1)$$

where

$$R' = R_0(\Delta) + \delta_2(\Delta)Y_{20}(\theta, \phi) \quad (2)$$

depends on the polar angles  $(\theta, \phi)$  between the nuclear symmetry axis and a point on its surface. In Eq. (2) the undeformed radius  $R_0(\Delta) = r_0(A_T^{1/3} + A_p^{1/3})$ , where  $A_T$  and  $A_p$  are target and projectile mass numbers. The symbol  $\Delta$  indicates the projectile size; to lowest order in  $\Delta/R_0$  both  $R_0$  and the quadrupole deformation length  $\delta_2(\Delta)$  are independent of  $\Delta$  Refs. 7, 13). Also, the nuclear potential deformation  $\beta_2^n$  is obtained from

$$\delta_2(0) = \beta_2^n r_0 A_T^{1/3}. \quad (3)$$

TABLE I. Coupled-channel parameters and nuclear potential deformations.

Target	Projectile	Energy (lab) (MeV)	$V_0$ (MeV)	$r_0$ (fm)	$a_0$ (fm)	$W$ (MeV)	$a_w$ (fm)	$\beta_2^n$
$^{24}\text{Mg}$	$^{12}\text{C}$	25, 30	36.0	1.20	0.52	4.0	0.52	0.29
	$^{16}\text{O}$	36	22.0	1.31	0.49	4.0	0.38	0.23
$^{28}\text{Si}$	$^{12}\text{C}$	30	41.0	1.20	0.52	4.2	0.52	-0.29
	$^{16}\text{O}$	33	18.0	1.31	0.49	4.0	0.38	-0.25
	$^{16}\text{O}$	36	22.0	1.31	0.49	4.0	0.38	-0.23
	$^{16}\text{O}$	38	23.0	1.31	0.49	4.0	0.38	-0.21
	$^{18}\text{O}$	36	22.0	1.31	0.49	6.0	0.38	-0.27

The Coulomb potential,  $V_C(r)$  in Eq. (1), is generated from the deformed charge density

$$\begin{aligned} \rho(r, \theta) &= \rho_0, \quad r \leq R_C(\theta) \\ &= 0, \quad r > R_C(\theta), \end{aligned} \quad (4)$$

where

$$R_C(\theta) = 1.2A_T^{1/3}[1 + \beta_2^c Y_{20}(\theta, \phi)] \text{ fm} \quad (5)$$

and the charge density is normalized to  $Ze$ . The parametrization of  $R_C$  by  $A_T^{1/3}$ , rather than by  $(A_T^{1/3} + A_p^{1/3})$ , has been shown previously<sup>11</sup> to give a better description of the double-folded Coulomb potential of two heavy ions.<sup>23</sup>

For the elastic scattering, no extensive searches over OM potential parameters were undertaken, since the main emphasis was to study inelastic scattering. The fits to the inelastic cross sections and the extracted deformation lengths are relatively insensitive to OM parameters, provided that they describe the elastic-scattering cross sections adequately.

For  $^{12}\text{C} + ^{24}\text{Mg}$  and  $^{12}\text{C} + ^{28}\text{Si}$  a four-parameter potential with  $a_w = a_0$  was sufficient to describe the elastic-scattering cross sections. In the  $^{16}\text{O} + ^{24}\text{Mg}$ ,  $^{16}\text{O} + ^{28}\text{Si}$ , and  $^{18}\text{O} + ^{28}\text{Si}$  scattering a six-parameter OM potential was necessary. The OM parameters are given in Table I.

The inelastic scattering was analyzed by coupled-channels calculations for  $0^+ - 2^+$  with quadrupole deformation only, as indicated in Eqs. (2) and (5). At the energies used the  $2^+$  cross sections are not very sensitive to hexadecapole ( $\beta_4$ ) deformations or to coupling to the  $4^+$  states.<sup>4</sup> For both  $^{24}\text{Mg}$  and  $^{28}\text{Si}$  axial symmetry was assumed, the evidence for axial asymmetry in  $^{24}\text{Mg}$  being weak.<sup>22</sup> The charge deformations  $\beta_2^c$  were chosen to be consistent with  $B(E2\uparrow)$  values which are related to charge densities by

$$[B(E2\uparrow)]^{1/2} = \int \rho(r, \theta) r^2 Y_{20}(\theta, \phi) d\vec{r}.$$

The  $B(E2\uparrow)$  values used were  $420 e^2 \text{ fm}^4$  for  $^{24}\text{Mg}$  (Ref. 24) and  $314 e^2 \text{ fm}^4$  for  $^{28}\text{Si}$  (Ref. 25). Equa-

tions (4)–(6) lead to  $\beta_2^c = 0.498$  for  $^{24}\text{Mg}$  and  $\beta_2^c = 0.466$  for  $^{28}\text{Si}$ , with the signs chosen consistent with measurement quadrupole moments<sup>26</sup> of the  $2^+$  states. The CC calculations used the code ECIS (Ref. 27) with 80 partial waves and radial integrations carried out to 40 fm to account correctly for Coulomb excitation. The parameters  $V$ ,  $W$ , and  $\beta_2^n$  were varied respectively from elastic-scattering and charge values to optimize the fits to the  $0^+$  and  $2^+$  cross sections shown in Figs. 2–6. The resulting potentials and deformations are given in Table I.

#### IV. RESULTS

##### $^{12}\text{C} + ^{24}\text{Mg}$

The measured and fitted cross sections for scattering to the ground and lowest  $2^+$  (1.37-MeV) states of  $^{24}\text{Mg}$  at  $^{12}\text{C}$  bombarding energies of 25 and 30 MeV are shown in Fig. 2. The same OM parameters and  $\beta_2^n$  values (Table I) yield good fits at both energies. The best-fit quadrupole deformation length  $\delta_2 = 1.80$  fm is in fair agreement with a previous measurement at 21 and 24 MeV (Ref. 11),  $\delta_2 = 1.55$  fm, and with systematics from a wide range of projectiles,<sup>13</sup> including projectile size effects,  $\delta_2 = 1.48 \pm 0.24$  fm. The prediction of the  $2^+$  cross section at 30 MeV using this value of  $\delta_2$ , shown dashed in Fig. 2, is clearly inferior to the best-fit value.

##### $^{16}\text{O} + ^{24}\text{Mg}$

The previously measured<sup>15</sup> cross sections for scattering to the ground and first-excited  $2^+$  (1.37-MeV) states of  $^{24}\text{Mg}$  at an  $^{16}\text{O}$  bombarding energy of 36 MeV are shown in Fig. 3. The OM parameters (Table I) used to describe the elastic scattering are similar to those in Ref. 15. The parameters obtained from the present CC analysis, which includes Coulomb excitation correctly, are given in Table I. Although good fits to the data were reported previously in Ref. 15, which did not include Coulomb excitation properly, the extracted

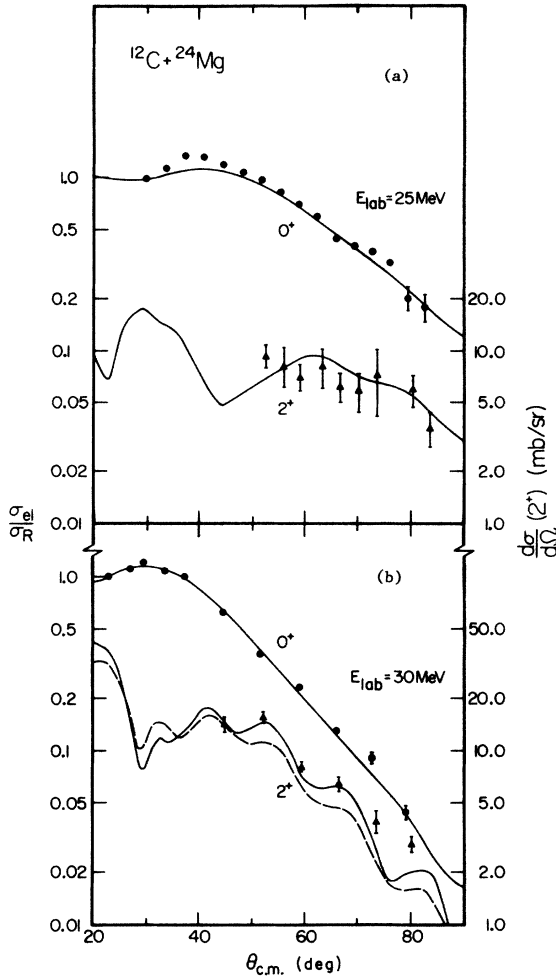


FIG. 2. Measured (indicated by dots and triangles) and fitted (solid curves) differential cross sections for scattering to the ground and lowest  $2^+$  (1.37-MeV) states of  $^{24}\text{Mg}$  at  $^{12}\text{C}$  bombarding energies of (a)  $E_{\text{lab}} = 25 \text{ MeV}$  and (b)  $E_{\text{lab}} = 30 \text{ MeV}$ . The error bars show statistical errors. The upper curves are the elastic cross sections, given as the ratio to Rutherford scattering  $\sigma/\sigma_{\text{R}}$ , while the lower curves are the inelastic-scattering cross sections. The dashed curve is a prediction from systematics, as discussed in Sec. IV.

$\delta_2 = 2.20$ . The reason for this large  $\delta_2$  was that the nuclear scattering contribution had to be increased to compensate for the too-small contribution from Coulomb excitation in order to fit the experimental cross sections. The best-fit deformation length  $\delta_2 = 1.63 \text{ fm}$  is in good agreement with the value extracted in the bombarding energy range  $E_{\text{lab}} = 28\text{--}33 \text{ MeV}$  (Ref. 11),  $\delta_2 = 1.55 \text{ fm}$ , with the value from  $E_{\text{lab}} = 20$  to  $42 \text{ MeV}$  (Ref. 4),  $\delta_2 = 1.83 \text{ fm}$ , with the value from a coupled-channels analysis at  $42 \text{ MeV}$  (Ref. 29),  $\delta_2 = 1.69 \text{ fm}$ , with an analysis at  $E_{\text{lab}} = 60 \text{ MeV}$  (Ref. 28),  $\delta_2 = 1.18 \text{ fm}$ , and

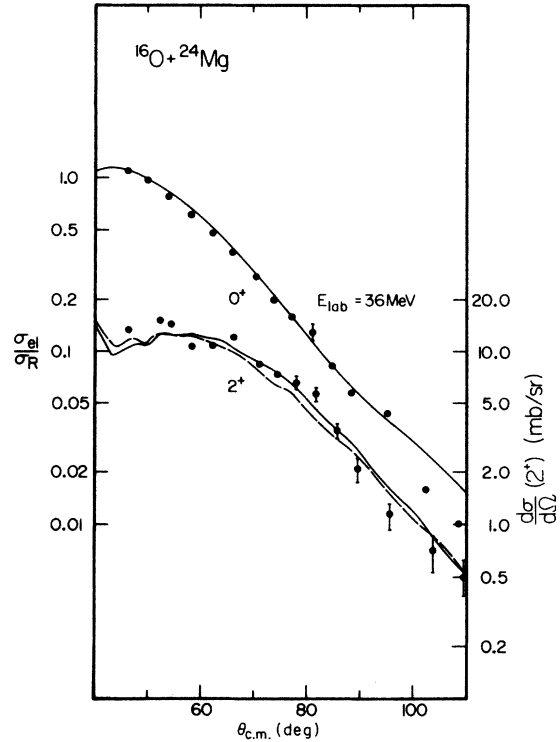


FIG. 3. Data from Ref. 15 (indicated by dots) and fits (solid curves) to differential cross sections for scattering to the ground and lowest  $2^+$  states of  $^{24}\text{Mg}$  by  $^{16}\text{O}$  at an  $^{16}\text{O}$  bombarding energy of  $36 \text{ MeV}$ . The upper curve is for elastic scattering shown as the ratio to Rutherford scattering  $\sigma/\sigma_{\text{R}}$ . The lower curve shows the inelastic cross section. The dashed curve, predicted from systematics, is discussed in Sec. IV.

with systematics,<sup>13</sup> including projectile-size effects,  $\delta_2 = 1.48 \pm 0.24 \text{ fm}$ . The predictions of this value, shown dashed in Fig. 3, give fits to the  $2^+$  cross section which are similar to the best fits.

#### $^{12}\text{C} + ^{28}\text{Si}$

The measured and calculated cross sections for scattering to the ground and first-excited  $2^+$  (1.78-MeV) states of  $^{28}\text{Si}$  by  $^{12}\text{C}$  at a bombarding energy of  $30 \text{ MeV}$  are shown in Fig. 4. The OM potential parameters are similar to those used for the  $^{12}\text{C} + ^{24}\text{Mg}$  scattering. The best-fit deformation length  $\delta_2 = 1.85 \text{ fm}$ , whereas an analysis at  $E_{\text{lab}} = 41.4 \text{ MeV}$  (Ref. 6) has obtained  $\delta_2 = -1.34 \text{ fm}$ , and systematics<sup>13</sup> (with finite-projectile-size corrections) indicate  $\delta_2 = -1.43 \pm 0.19 \text{ fm}$ . This value predicts the dashed curve in Fig. 4, which is less than the data at all angles, typically by 25%, which is of the order of the difference in  $\delta_2$  values.

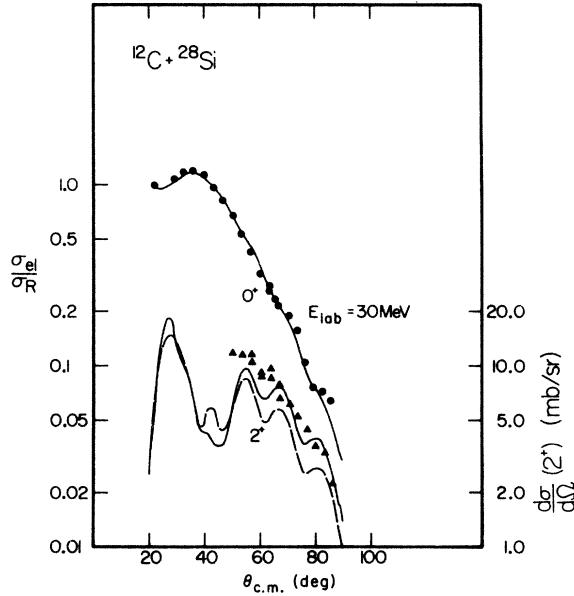


FIG. 4. Measured (indicated by dots and triangles) and fitted (solid curves) differential cross sections for scattering to the ground and lowest  $2^+$  (1.78-MeV) states of  $^{28}\text{Si}$  by  $^{12}\text{C}$  at a  $^{12}\text{C}$  bombarding energy of 30 MeV. The upper curve is the elastic scattering cross section given as the ratio to Rutherford scattering  $\sigma/\sigma_R$ . The lower curve shows the inelastic scattering cross section. The dashed curve is a CC prediction from systematics of deformation lengths, as discussed in Sec. IV.

### $^{16}\text{O} + ^{28}\text{Si}$

The previously measured<sup>16</sup> cross sections for  $^{16}\text{O}$  scattering at bombarding energies of 33.0, 36.0, and 38.0 MeV to the ground and first-excited  $2^+$  (1.78-MeV) states of  $^{28}\text{Si}$  are shown in Fig. 5. The elastic-scattering OM parameters obtained in the present reanalysis are very similar to those in Ref. 16, and give comparable fits to those obtained in an energy-independent analysis<sup>30</sup> for  $E_{\text{lab}} = 33\text{--}215$  MeV. The inelastic cross sections exhibit strong nuclear-Coulomb interference, the minimum of which moves to forward angles as the bombarding energy increases, although Coulomb excitation is important at all angles. The calculated cross sections reported in Ref. 16 did not include any contribution from Coulomb excitation. As in the case of  $^{16}\text{O} + ^{24}\text{Mg}$  scattering the extracted  $\delta_2$  in Ref. 16 is too large by 30%. Also, for the  $^{16}\text{O} + ^{28}\text{Si}$  scattering reported in Ref. 16, the noninclusion of Coulomb excitation precludes fitting the cross sections at forward angles in the region of strong nuclear-Coulomb interference in contrast to the fits presented here. We obtain  $\delta_2 = -1.70 \pm 0.15$  fm for the mean and standard deviation among the three bombarding energies. Systematics,<sup>13</sup> with finite-projectile-size corrections,<sup>7</sup>

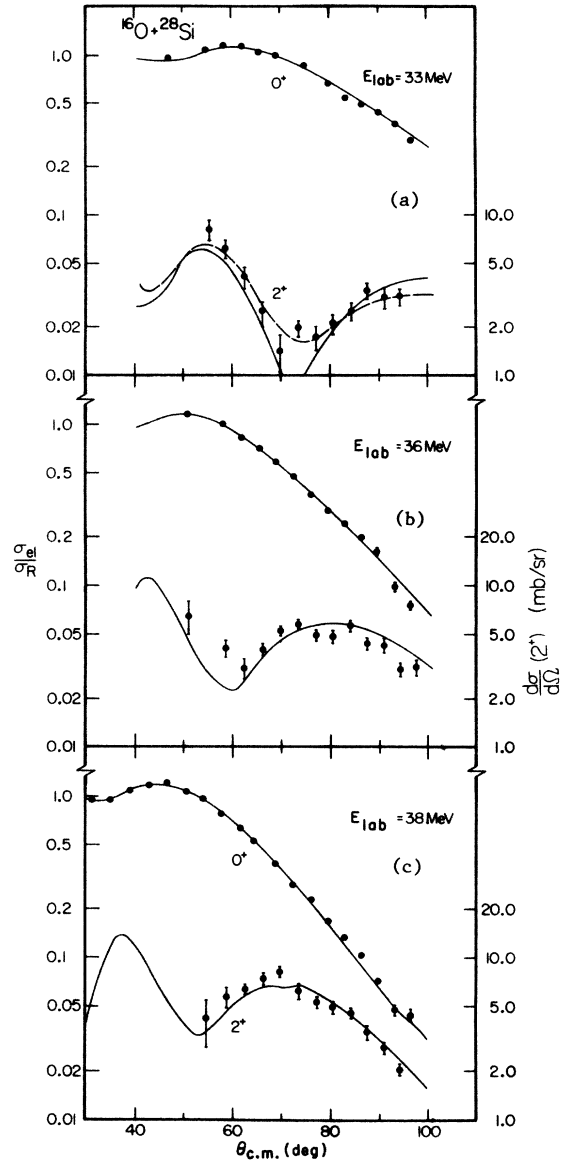


FIG. 5. Data from Ref. 16 (indicated by dots) and fitted (solid curves) differential cross sections for scattering to the ground and lowest  $2^+$  (1.78-MeV) of  $^{28}\text{Si}$  by  $^{16}\text{O}$  at  $^{16}\text{O}$  bombarding energies of  $E_{\text{lab}} = 30, 33, 36,$  and  $38$  MeV. In (a), (b), and (c) the upper curve is the elastic cross section expressed as the ratio to Rutherford scattering  $\sigma/\sigma_R$  and the lower curve is the inelastic scattering cross section. The CC analysis is discussed in Sec. IV. The dashed curve in (a) is a prediction from systematics.

predict  $\delta_2 = -1.43 \pm 0.19$  fm, which produces the  $2^+$  cross section at 33 MeV shown dashed in Fig. 5(a).

### $^{18}\text{O} + ^{28}\text{Si}$

Previously measured<sup>16</sup> cross sections for  $^{18}\text{O}$  scattering from the ground and first-excited (1.78-

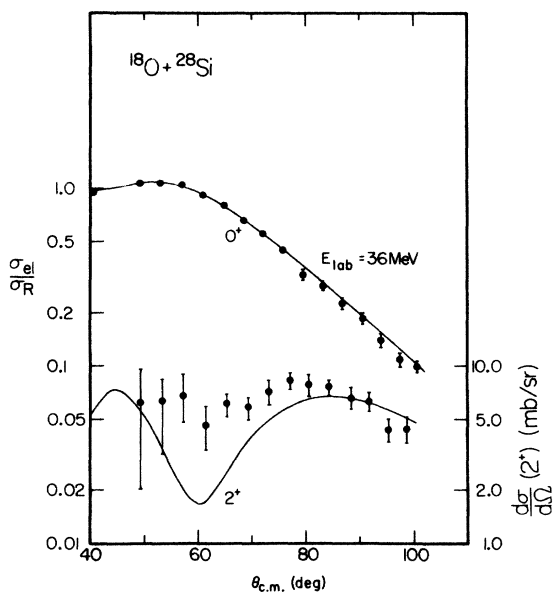


FIG. 6. Data from Ref. 16 (indicated by dots) and fitted (solid curves) differential cross sections for scattering to the ground and lowest  $2^+$  states of  $^{28}\text{Si}$  by  $^{18}\text{O}$  at an  $^{18}\text{O}$  bombarding energy of 36 MeV. The upper curve is the elastic scattering cross section expressed as the ratio to Rutherford scattering  $\sigma/\sigma_R$ . The lower curve is the inelastic cross section and includes inelastic scattering to the first-excited state of  $^{18}\text{O}$ . The CC analysis is discussed in Sec. IV.

MeV) states of  $^{28}\text{Si}$  at a bombarding energy of 36 MeV are shown in Fig. 6. The fit to the inelastic cross section is much poorer than for the other data reported here. This is probably due to the contamination of the inelastic spectrum by scattering to the lowest  $2^+$  (1.98-MeV) state of  $^{18}\text{O}$ , which, with the experimental resolution of 500 keV, is unresolved from the first-excited state of  $^{28}\text{Si}$ . Recent measurements of  $^{18}\text{O}+^{16}\text{O}$  scattering<sup>31</sup> at similar energies indicate strong excitation of this

state in  $^{18}\text{O}$ . Therefore, the extracted deformation length of  $\delta_2 = -2.0$  fm gives an upper limit on the magnitude of  $\delta_2$ . It is larger than the weighted mean  $\delta_2 = -1.77 \pm 0.07$  fm obtained from the  $^{12}\text{C}$  and  $^{16}\text{O}$  bombardments.

## V. DISCUSSION AND SUMMARY

The potential quadrupole deformation lengths  $\delta_2$  have been extracted for  $^{12}\text{C}$  and  $^{16}\text{O}$  bombardment of  $^{24}\text{Mg}$  and  $^{28}\text{Si}$  at several energies near the Coulomb barrier. We find average values (with standard deviations) of  $\delta_2 = 1.72 \pm 0.09$  fm for  $^{24}\text{Mg}$ , and  $\delta_2 = -1.77 \pm 0.07$  fm for  $^{28}\text{Si}$ , which are, in magnitude, about one standard deviation greater than systematics<sup>13</sup> predict. The errors reported for the extracted  $\delta_2$  parameters are due to the dominance of Coulomb excitation in the inelastic cross sections and small changes in  $\delta_2$  do not significantly alter the calculated fits to the measured cross sections. However, the predictions for  $^{12}\text{C}$  and  $^{16}\text{O}$  projectiles are essentially extrapolations from values obtained for  $A_p < 12$ .

Although the extracted nuclear quadrupole deformation parameters differ from the Coulomb deformation parameters, the quadrupole moments deduced from them are essentially in agreement.<sup>13</sup> Remaining discrepancies may be attributed to the nuclear model assumptions used: (1) The first two states in  $^{24}\text{Mg}$  and  $^{28}\text{Si}$  have been represented as those of ideal rotational nuclei. (2) The charge distribution used to calculate the Coulomb excitation has a sharply defined surface rather than a diffuse edge, which could produce small effects in the nuclear-Coulomb interference minima. Higher-order corrections to the coupled-channels analysis, such as the inclusion of  $\beta_4$  deformations, would be justified only by including data for the  $4^+$  states, by improving the absolute cross section measurements, and by extending the data to more backward angles.

†Supported in part by the Division of Physical Research, U. S. Energy Research and Development Administration and by National Science Foundation Grant, PHY76-08788.

\*Present address: Pfizer Medical Systems, Inc., 9052 Old Annapolis Road, Columbia, Maryland 21045.

‡Permanent Address: Department of Physics and Astronomy, University of North Carolina at Chapel Hill, Chapel Hill, North Carolina 27514.

<sup>1</sup>I. Y. Lee, J. X. Saladin, J. Holden, J. O'Brien, C. Baktash, C. Bemis, Jr., P. H. Stelson, F. K. McGowan, W. T. Miller, J. L. C. Ford, Jr., R. L. Robinson, and W. Tuttle, *Phys. Rev. C* **12**, 1483 (1975), and references therein.

<sup>2</sup>W. Brückner, D. Husar, D. Pelte, K. Traxel, M. Sam-

uel, and U. Smilansky, *Nucl. Phys.* **A231**, 159 (1974).

<sup>3</sup>F. Videbaek, P. R. Christensen, O. Hansen, and K. Ulbak, *Nucl. Phys.* **A256**, 301 (1976).

<sup>4</sup>J. X. Saladin, I. Y. Lee, R. C. Haight, and D. Vitoux, *Phys. Rev. C* **14**, 992 (1976).

<sup>5</sup>G. R. Satchler, in *Reactions Between Complex Nuclei*, edited by R. L. Robinson, F. K. McGowan, J. B. Ball, and J. H. Hamilton (North-Holland, 1974), Vol. 2, p. 171.

<sup>6</sup>F. Todd Baker, Alan Scott, E. E. Gross, B. C. Hensley, and D. L. Hillis, *Nucl. Phys. A* (to be published).

<sup>7</sup>D. L. Hendrie, *Phys. Rev. Lett.* **31**, 478 (1973).

<sup>8</sup>H. Rebel, in *Radial Shape of Nuclei*, edited by A. Budzanowski and A. Kapuscik (Jagellonian University, Institute of Nuclear Physics, Cracow, 1976),

- p. 163.
- <sup>9</sup>H. Fischer, D. Kamke, H. J. Kittling, E. Kuhlmann, H. Plicht, and R. Schormann, *Phys. Rev. C* **15**, 921 (1977).
- <sup>10</sup>T. Cooper, W. Bertozzi, J. Heisenberg, S. Kowalski, W. Turchinetz, C. Williamson, L. Cardman, S. Fivovzinsky, J. Lightbody, Jr., and S. Penner, *Phys. Rev. C* **13**, 1083 (1976).
- <sup>11</sup>J. Carter, R. G. Clarkson, V. Hnizdo, R. J. Keddy, and D. W. Mingay, *Nucl. Phys.* **A273**, 523 (1976).
- <sup>12</sup>K. E. Rehm, H. J. Körner, M. Richter, H. P. Rother, J. P. Schiffer, and H. Spieler, *Phys. Rev. C* **12**, 1945 (1975).
- <sup>13</sup>W. J. Thompson and J. S. Eck, *Phys. Lett.* **67B**, 151 (1977).
- <sup>14</sup>R. H. Siemssen, in *Nuclear Spectroscopy and Reactions*, edited by J. Cerny (Academic, New York, 1974), Part. B, p. 233.
- <sup>15</sup>J. S. Eck and W. J. Thompson, in *Nuclear Reactions Induced by Heavy Ions*, edited by R. Bock and W. R. Hering (North-Holland, Amsterdam, 1970), p. 85.
- <sup>16</sup>D. S. Gale and J. S. Eck, *Phys. Rev. C* **7**, 1950 (1973).
- <sup>17</sup>G. W. Hartnell, J. C. Legg, J. R. Macdonald, and G. C. Seaman, in *Proceedings of the Symposium on Ion Sources and Formation of Ion Beams*, Brookhaven National Laboratory, 1971 (unpublished), p. 285.
- <sup>18</sup>J. S. Eck and D. O. Elliott, *Nucl. Instrum. Methods* **121**, 411 (1974).
- <sup>19</sup>I. Takayanagi, M. Katsuta, K. Katori, and R. Chiba, *Nucl. Instrum. Methods* **45**, 345 (1966).
- <sup>20</sup>A. Bohr and B. R. Mottelson, *Nuclear Structure* (Benjamin, Reading, Massachusetts, 1975), Vol. 2, p. 1.
- <sup>21</sup>T. Tamura, *Rev. Mod. Phys.* **37**, 678 (1965).
- <sup>22</sup>P. Mpanias and M. L. Rustgi, *Phys. Rev. C* **14**, 365 (1976).
- <sup>23</sup>R. M. DeVries and M. R. Clover, *Nucl. Phys.* **A243**, 528 (1975).
- <sup>24</sup>S. F. Biagi, W. R. Phillips, and A. R. Barnett, *Nucl. Phys.* **A242**, 160 (1975); D. Branford, A. C. McGough, and I. F. Wright, *ibid.* **A241**, 349 (1975); A. Nakada and Y. Torizuka, *J. Phys. Soc. Jpn.* **32**, 1 (1972).
- <sup>25</sup>Y. Horikawa, *Prog. Theor. Phys. Jpn.* **47**, 867 (1972); P. M. Endt and C. van der Leun, *Nucl. Phys.* **A214**, 1 (1973).
- <sup>26</sup>O. Häusser, in *Nuclear Spectroscopy and Reactions*, edited by J. Cerny (see Ref. 14), Part C, p. 55.
- <sup>27</sup>J. Raynal, computer program *ecis* (unpublished).
- <sup>28</sup>K. Siwek-Wilczynska, J. Wilczynski, and P. R. Christensen, *Nucl. Phys.* **A229**, 461 (1974).
- <sup>29</sup>B. T. Chait and D. Sinclair, *Nucl. Phys.* **A279**, 517 (1977).
- <sup>30</sup>J. G. Cramer, R. M. DeVries, D. A. Goldberg, M. S. Zisman, and C. F. Maguire, *Phys. Rev. C* **14**, 2158 (1976).
- <sup>31</sup>R. Vandenbosch (private communication).
- <sup>32</sup>G. Thomas, in *Jahresbericht, Dynamitron Tandem laboratorium*, Bochum, 1975 (unpublished), p. 44.